Title

Interferometric SAR modelling of near surface data to improve geological model in the Surat Basin, Australia

Authors

Moghaddam, Negin Fouladi

Nourollah, Hadi

Vasco, Donald W

et al.

Publication Date

2021-11-01

DOI

10.1016/j.jappgeo.2021.104444

Peer reviewed

Interferometric SAR modelling of near surface data to improve geological model in the Surat Basin, Australia

Negin Fouladi Moghaddam[1*], Hadi Nourollah[2], Donald W. Vasco[3], Sergey V. Samsonov[4]
Christoph Rudiger[5]

[1] Research School of Earth Sciences, The Australian National University, Canberra, Australia

Negin.moghaddam@anu.edu.au

Negin.moghaddam@monash.edu

[2]Panorama Petroleum Pty Ltd., Melbourne, Australia

hadi@panopetro.com

[3]Lawrence Berkeley National Lab, Energy Geosciences, Berkeley, California, USA

dwvasco@lbl.gov

[4] Canada Centre for Mapping and Earth Observation, Natural Resources Canada, Ottawa, Canada

sergey.samsonov@canada.ca

[5]Department of Civil Engineering, Monash University, Melbourne, Australia

Chris.Rudiger@monash.edu

SUMMARY

This paper presents a study on geophysical inverse modelling for sub-surface structural properties of an unconventional hydrocarbon site that was monitored previously by Interferometric Synthetic Aperture Radar (InSAR) technology for surface deformation. A static three-dimensional geomodel along with extracted property maps replicates the depth of each underlying stratigraphic unit and structural feature with the density of each geological layer. We examine the hypothesis that integration of elastic properties of each formation layer with InSAR observations in a stratified elastic medium will lead to a viscoelastic geophysical inverse problem that can be solved to estimate fractional volume change at the reservoir level. Moreover, we examine synthetic scenarios in which the elastic properties of the formations are perturbed before determining the resulting impact on the rate of surface deformation. The results show that although the slope of underlying formations, their density and depth can define the extent and pattern of a deformation signal, their properties have a marginal impact on volumetric change compared to the dense network of shallow depth Coal Seam Gas(CSG) mining wells. Besides, it is also demonstrated that the inversion of InSAR deformation maps can resolve the uncertainties associated with low-resolution seismic interpretation as well as filling the data gaps within seismic acquisitions. A significant contribution of this investigation to the geological basin modelling involves a) introducing a remote and non-invasive technology such as InSAR to improve geophysical mapping of subsurface structures such as faults in areas with sparse or no reflective seismic information, and b) applying a multi-layer viscoelastic geophysical source model for an unconventional hydrocarbon reservoir such as CSG.

KEYWORDS

Geophysical inverse modelling, Unconventional hydrocarbon, InSAR, Ground surface deformation, Seismic acquisitions, Subsurface structures

1 INTRODUCTION

Modelling subsurface structures and understanding reservoir characteristics are critical for the energy production, storing CO_2 emissions, and preserving groundwater supplies. Three-dimensional geological modelling or geomodelling is the numerical equivalent of a geological map that describes the physical quantities in the domain of interest (Mallet, 2008). In general, the structural framework (i.e. resolution and maximum cell size), rock type, reservoir quality including its porosity and permeability, and geostatistics are the components of a static geological model (Ezekwe, 2011), that can then be used as a benchmark for reservoir dynamic modelling or flow simulation.

Conventionally, integration of *in-situ* measurements such as lithological, structural, and geophysical datasets with a quantitative approach will result in a three-dimensional numerical equivalent of the subsurface, which constrains exploration targets at depth, and extracts valuable information for reservoir management (Fallara *et al.* 2006). However, a major challenge in building geological models is the availability of the subsurface information at different resolutions and the possibility of multiple geological interpretations that lead to uncertainties in reservoir characteristics (Al-Khalifa *et al.* 2007; Singh *et al.* 2013).

As part of the Great Artesian Basin, the Surat Basin is an onshore basin in Australia that mainly located in the state of Queensland while its southern boundary extends to the New South Wales. Some of the layers in this Basin are porous aquifers, which are accessed for groundwater supply while below the main aquifers, denser and less permeable Walloon Coal Measures (WCM) hosts the CSG shallow reservoirs. According to the report from Queensland Water Commission (QWC, 2012), depressurization in groundwater aquifers and associated gas leakages have the potential to reduce groundwater supply and discharge in the region, causing compaction of geological layers and resulting in ground surface subsidence.

Since geodetic observations such as levelling and GPS are not available or very sparse for independent monitoring of ground motion in this part of the Surat Basin, Interferometric SAR (InSAR) historical and non in-situ observations was used previously to map the ground surface deformation patterns and its locations. Using SBAS algorithm, available SAR images covering the proposed region processed

and then used to identify the optimal set of interferograms to extract ground surface deformation rate map (Moghaddam et al., 2016). This rate map will then constrain multi-layer viscoelastic model for a CSG reservoir to estimate volumetric changes in the reservoir level and to examine the resilience of the source model to variations in the properties of the reservoir layers.

To analyse the subsurface structure, a priori knowledge about the sequence and thickness of the stratigraphic layers and their relationship with controlling structures such as faults is essential for three-dimensional modelling. Static or dynamic modelling of geological units (i.e. geomodelling) consists of the rock matrix and/or the fluid flowing in its pore spaces (Hosseini et al., 2013). The static model is a detailed reconstruction of the geological structure of the reservoir (e.g. the shape of the layers and the trend of the faults), including definition of the geological zones and the petro-physical parameters (initial porosity and density) as a function of the location. Therefore, the result of a static study of reservoir and its surrounding region consists all geological, lithological, stratigraphical and petrophysical aspects (Adeoti et al., 2014).

As there is no unique solution for inverse problems, properly understanding the problem and determining a physically adequate deformation model by using available geological and geophysical information is essential. Time series of deformation signals in the proposed area show viscoelastic patterns in a region with flat Earth and stratified subsurface formations without particular geometrical shape for the source. Accordingly, for the case study in this research, a multi-layer viscoelastic source model (Vasco et al., 2008) will be applied as a numerical geophysical inversion method. This inversion technique is an approach that integrates both mathematical and physical principles for a particular problem in a coal-rich area. The constraints for this method are defined based on the physics of the problem in a multi-layer stratified medium with more than 350m thickness of overburden sediments and will play the most important role in the inversion process. They either can be hidden behind the inversion method such as slip distribution for shallow features or can add more convenience to the modelling procedure such as smoothing (Du et al., 1992).

In this paper, following a brief overview of the available data resources, we will discuss the subsurface geological model to calculate volumetric changes in the reservoir layer. Consequently, by

analysing the petrophysical attributes of the subsurface and InSAR-based displacement information, the spatial distribution of fractional volume change over the proposed area will be discussed.

2 DATA RESOURCES

The previous study in this part of the Surat Basin illustrated that using multi-temporal SAR observations for InSAR analysis (Table1) is a cost-efficient and reliable tool for the historical study of ground surface deformation where in-situ measurements are not available or sparse. The area of study in the north-western part of the Surat Basin, Australia covers an area of 35km by 35km. It was

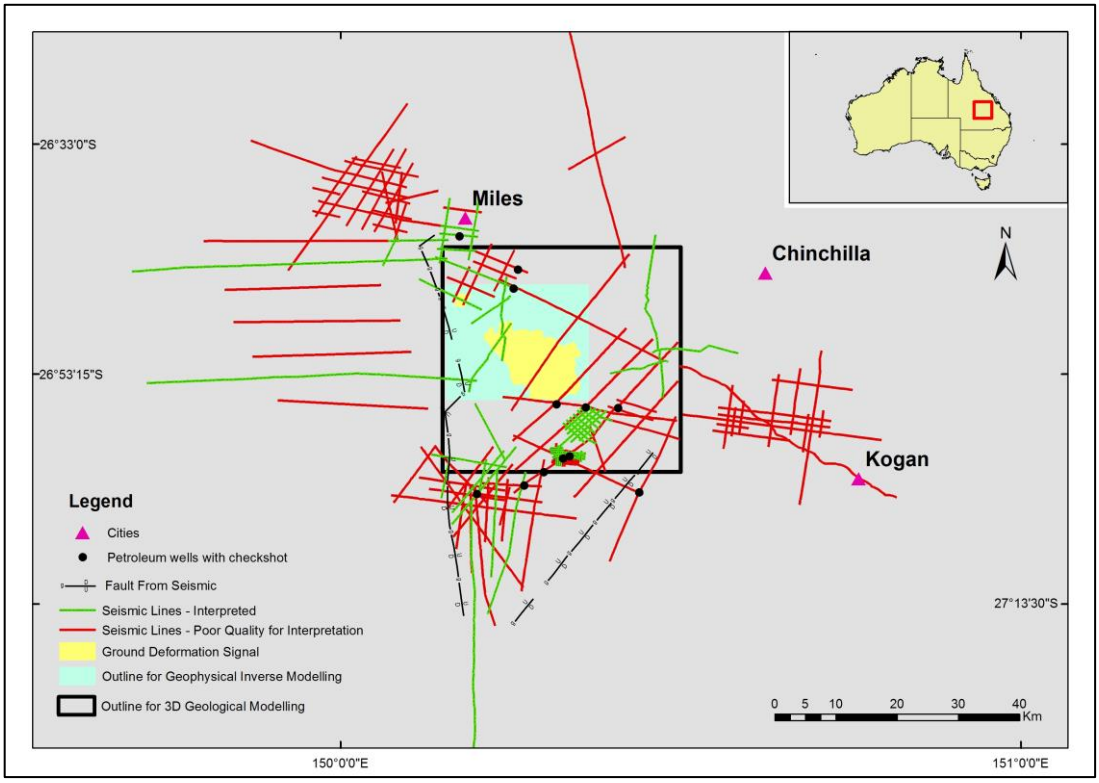

Figure 1. Outline of the area for which the 3D geological modelling and geophysical inverse modelling were undertaken (black outline), showing the available seismic dataset (green and red lines). The green seismic lines were in good quality for seismic interpretation but the red ones were in poor quality. The black dot points show the location of petroleum wells with velocity check shots.

previously studied using satellite imagery acquired by the Phased Array L-band SAR (PALSAR) on-board the Japanese Earth Exploration Agency's Advanced Land Observation Satellite (ALOS) (Moghaddam *et al.* 2016).

To screen the long-term behaviour of the ground surface and to estimate the rate of deformation in the focal area of the Surat Basin, a standard Differential InSAR processing including orbit correction, phase

unwrapping and geocoding for L-band SAR images with temporal and spatial baseline smaller than the predefined threshold values was performed. This was followed by the stacking technique for interferograms with high coherency and low unwrapping errors, to remove residual orbital ramps and long-wavelength atmospheric noise. Applying the stacking algorithm over this dataset and at the same time having a sufficient number of interferograms ultimately provided a better cumulative phase delay response with less noise contribution. Stacking results for each scene suggested that among the four ALOS-PALSAR scenes, both T365-F6630 and T366-F6640 have significant deformation signal patterns after 2007; however, T366-F6640 covering the area in the Surat Basin where 2D seismic information and petroleum well logs with checkpoints are sufficiently available. It is worth mentioning that when the proposed area was monitored by RADARSAT-2 acquisitions during 2012–2014, the ground surface in location A retained its deformation pattern experiencing downward motion. To estimate the accuracy of the InSAR deformation measurement for reliable inversion results, LOS linear deformation rates resulting from SBAS approach for each of the two datasets (i.e. T366-F6640 and T365-F6630 as one set each) were plotted for four different reference points. Details of this assessment are available in Moghaddam *et al.*, 2016. For T366-F6640 true subsidence in LOS was less than -0.68 cm/year while for T365-F6630 deformation values change between ±0.42 cm/year. Based on the initial processing results using stacking and predetermined deformation signals in the region, the SBAS code (Samsonov et al., 2011), as an advanced InSAR processing technique to solve for deformation rate and the residual topographic noise simultaneously, was applied for ALOS-PALSAR archived images. The analysis of ALOS-PALSAR observations is from 05 December 2006 through 01 March 2011 and includes different acquisition time frequencies for single (FBS) and dual beam (FBD) modes. To apply the SBAS approach, a parameter file consisting of all interferograms with high coherency, i.e. more than 0.3 was required. The most coherent interferograms for this purpose were selected by calculating the mean coherence of each interferogram. By using such an approach, the linear rate of deformation for both scenes and its corresponding error was generated.

Comparing the space-borne long-term satellite observation to CSG extraction rates, deformation scenarios in different locations have been proposed. This observation suggests that the detected subsidence signal may have resulted from volumetric changes in the subsurface formations and adjacent

overburden due to gas extraction and associated strata compaction, which can occur due to changes in pore pressure and stresses in rock matrix.

Table1. ALOS PALSAR data used for Differential InSAR processing in this work: time span (in YYYYMMDD format), azimuth θ and incidence angle ϕ, number of available SAR images and number of calculated interferograms.

InSAR set	Time span	Resolution(m)	θ(°)	ϕ(°)	N	M
ALOS, track 365, frame 6630 (asc)	20070103–20110301	4.7-3	-14.66	39	20	37
ALOS, track 365, frame 6640 (asc)	20070103–20110301	4.7-3	-14.58	39	20	38
ALOS, track 366, frame 6630 (asc)	20061205–20110131	4.7-3	-14.66	39	22	60
ALOS, track 366, frame 6640 (asc)	20061205–20110131	4.7-3	-14.58	39	22	61

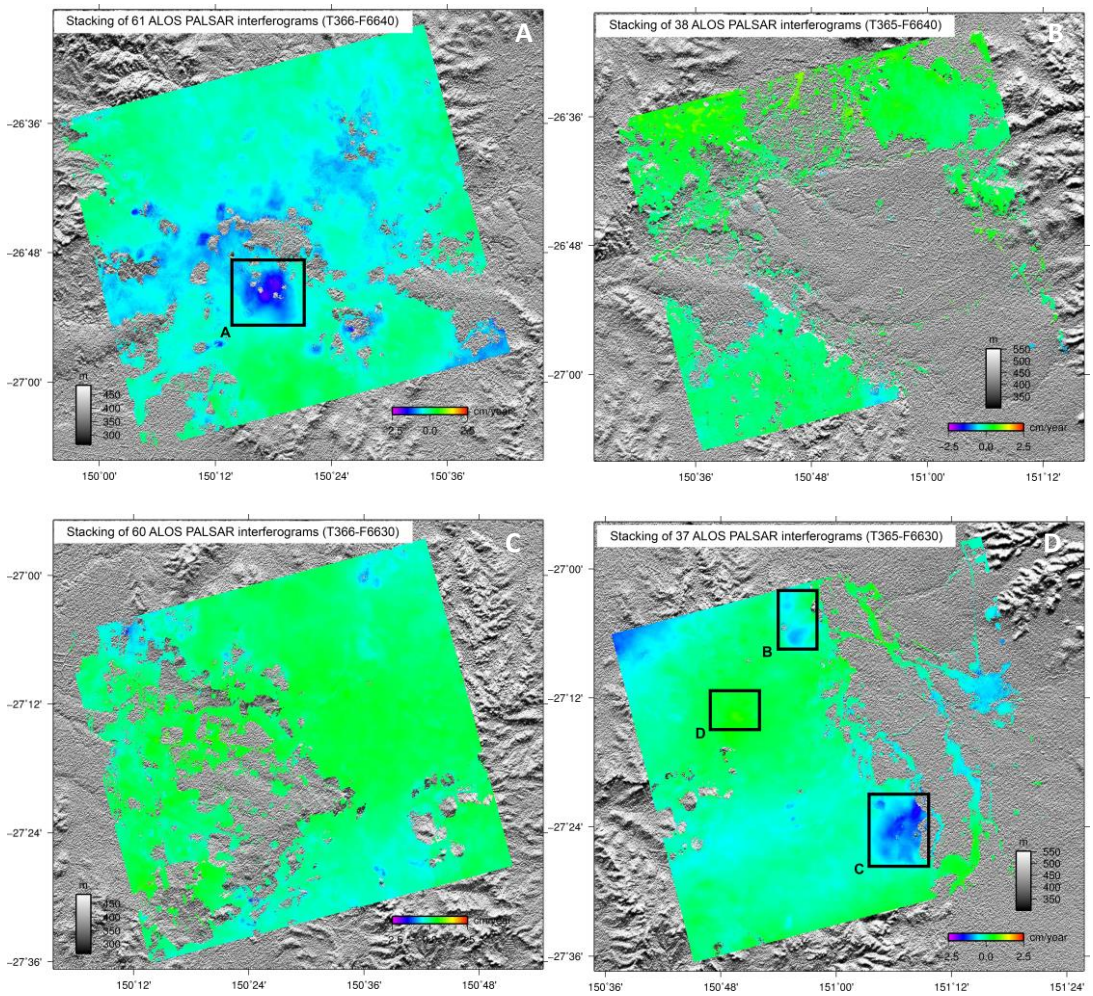

Figure 2. Line of sight deformation rates (cm/year) resulted from stacking of ALOS PALSAR ascending scenes. Based on processing results (Moghaddam et al., 2016), significant phase delay responses were detected in Track 366-Frame 6640 and Track 365-Frame6630. For geophysical inverse modelling location A with downward motion in Track 366 - Frame 6640 is a candidate site and closely aligned with CSG mining operations in this region.

Selection of the proposed region for seismic interpretation was based on the available seismic data, check shots, and their proximity to the deformation signal (i.e. location A) in Track 366 - Frame6640

detected by interferometric SAR analysis. According to the available dataset, there are 79 2D seismic lines with a total length of 893 km in the area of interest, while only 50 seismic lines in 10 different seismic surveys had the relevant quality and information (i.e. navigation file and shot point map) for uploading into the seismic interpretation package (i.e. Petrel Schlumberger ©). In addition to the 2D seismic acquisition, relevant geological and geophysical reports, as well as Seismic Reference Survey (SRS) were gathered. Generally, migrated seismic lines with spatial and temporal corrections that shift the signal to its originating location of reflectors are more preferable for seismic interpretation; however, in cases that the migrated lines were of poor quality, individual non-migrated lines were ordered and used for better quality interpretation. In addition to stratigraphic interpretation, seismic surveys can also be used for structural interpretation such as locating normal faults, strike-slip faults, reverse faults and thrust faults through defining regional stresses in the area of interest. Around 50 available wells in the area of interest have recorded formation tops, while 12 of these wells are located within the study area or in the vicinity (i.e. less than 2.5km) and are accompanied by SRSs. These SRSs or velocity check shots are designed as a calibration mechanism for reflection seismic data. Bottom-hole data from the 12 wells penetrating the basement (unconformity horizon) along with 112 CSG wells with wire-line logs and petrophysical information (porosity, density, shear and compressional velocity) were also used. Supplementary data such as well completion reports with accompanying information about exploration well location, measured depths, well casing and the historical status of the operation were also gathered from the Department of Natural Resources, Mines and Energy (DNRME) publicly available database. Although 14 groundwater observation wells provide some temporally sparse information about the groundwater level and conditions of the aquifer in this part of the Surat Basin, their acquisition periods are not continuous enough to cover the missing information in the geomodelling procedure. Unfortunately, in this study, there was no access to core plugs with measurements of porosity, directional permeability, compressibility and grain density for specific wells. In other words, the sparse distribution of data in this part of the Surat Basin presents a challenge for static geological modelling. The following section includes details of the parameters incorporated into subsurface geological modelling and geophysical inverse modelling. All the data sources for geological model development are listed in Table2:

Table2. List of in situ measurements for 3D geological modelling for the proposed area in the Surat Basin. These data sources are publically available in different scales.

Data	Name	Source
Surface Elevation	ASTER DEM with 30m resolution S25E148	http://gdem.ersdac.jspacesystems.or.jp/search.jsp
Surface Geology	Geological Map of Queensland (2012), scale 1:2,000000	Geological Survey of Queensland
Seismic Surveys	50 2D seismic lines in 10 different surveys	Geological Survey of Queensland
Well Logs	112 CSG and 12 Petroleum Well	Department of Natural Resources, Mines and Energy

3 METHODOLOGY

3.1 Subsurface Geological Modelling

Static geological modelling to assess the structural properties and characterize shallow depth aquifers in the Surat Basin is critical for having a holistic image of the subsurface with assigned petrophysical properties. It can also be used as a basis for dynamic geo-modelling and fluid flow simulation in the same area.

Interpretation of seismic data helps define the subsurface structural framework where faults and stratigraphic units (Fig.3) can be mapped. The petrophysical properties of the rock units such as porosity, permeability, and water saturation may be directly derived from the downhole log data of petroleum and CSG wells (Wickens and Bouma, 2000; Ezekwe and Filler, 2005; McCarthy *et al.* 2006).

The primary objective of developing a three-dimensional geological model is to have a realization of the subsurface, which honours the available dataset at known points and provides a robust interpretation between these points for the full extent of the model. This framework can then be filled with petrophysical attributes to define the properties of the subsurface, which will be an input to the geophysical inversion using InSAR observations of surface deformation. The extent of the model is defined based on the spatial pattern of surface deformation and seismic data availability (Fig.1). The seismic interpretation including horizon and fault interpretation is followed by building a 3D velocity model to develop a depth geological model within the area of interest.

The study area in the Surat Basin has poor 2D seismic data coverage and no 3D seismic data. Having a good quality seismic section with suitable vertical resolution provides an initial picture of the main structural features and underlying stratigraphic sequences; however, in practice, this is not always

possible. Furthermore, the noise level of several seismic lines obscures the key subsurface reflectors, thus making the interpretation difficult. Interpretation of stratigraphic layers and structural faults using 2D seismic acquisitions is conducted in the time domain, while subsurface geological features are in the depth domain. The link between time and depth is through velocity modelling (Cameron *et al*. 2006). Therefore, to convert the time model to depth, a velocity model is constructed.

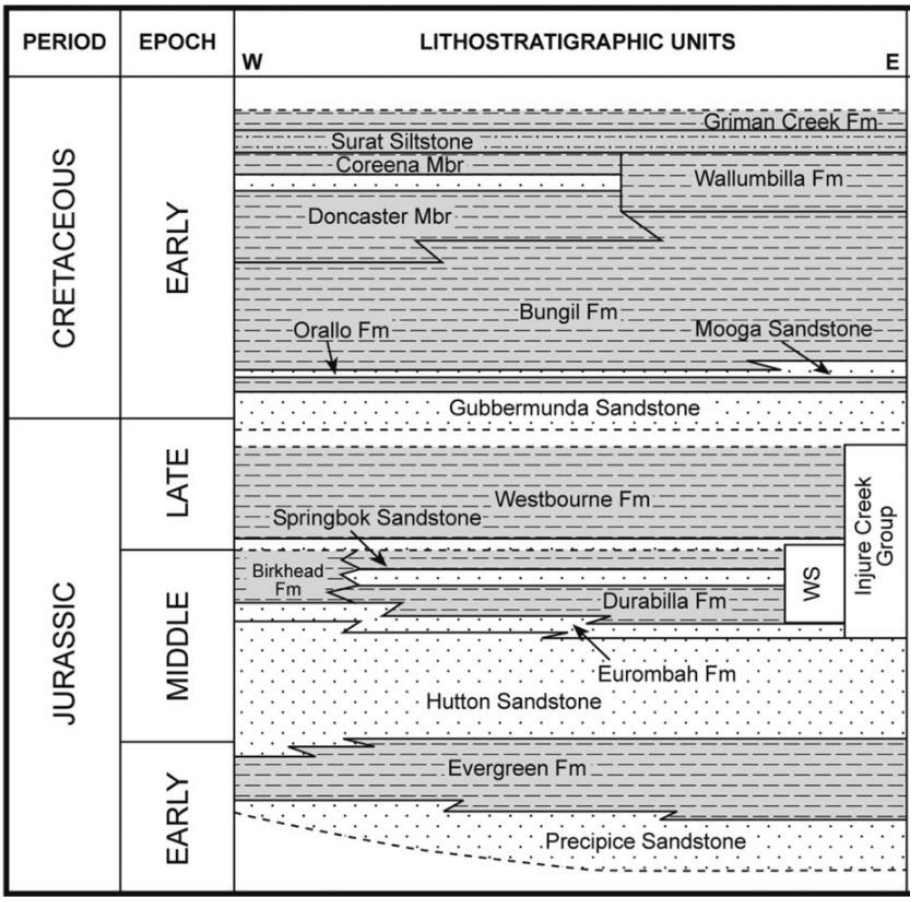

Figure 3. Simplified stratigraphy of the Surat Basin, Australia Modified after [Martin et al., 2013]

There are two approaches to build a geological model in depth domain. The first method is to build a model in the time domain and then convert it into depth domain using the velocity model. The second method is to convert selected horizons and faults directly from time to depth domain using a velocity model and subsequently build a 3D geological model (Yilmaz, 2001). In this study, both methods were examined. Lack of full seismic coverage to build a reliable Two-way Travel Time (TWT) structural model and limited velocity information proved the second method to produce better results.

The velocity model for the area of study utilised three horizons: the Walloon Coal Measures, the Hutton Sandstone, and the Basement. The velocity model is capped by the digital terrain model (DTM) and corrected by formation tops at wells for the above-mentioned stratigraphic levels. Interval velocities for each level is calculated using equation 1:

$$V_{Int} = \text{isochore(depth)}/\text{isochron(time)} \quad (1)$$

The depth surfaces were generated by introducing the velocity model to the surfaces in time, and the time horizons were converted to structural horizons in order to produce depth surfaces. The depth surfaces combined with depth-converted structural faults to produce a structural model. A comparison of this model against well top locations presented a good match between stratigraphic well tops and seismic horizons in the initial seismic interpretation stage.

In order to generate a homogenous distribution of petrophysical properties between the available wells and to preserve the reservoir heterogeneity, wire-line logs such as Sonic, Neutron Porosity (NPOR), Density (DEN), Gamma Ray (GR), and Spontaneous Potential (SP) were used for property modelling. Alternatively, to make sure that the initial assumption is correct, a spherical variogram was used to determine the range and the nugget of the petrophysical attribute and the property estimation was conducted using the default variogram distribution.

3.2 Geophysical Inverse Modelling

In order to interpret the surface deformation in terms of volume change at depth, we need to embed the reservoir in an elastic structural model. The numerical source model PSGRN/PSCMP (Wang *et al.* 2006) was used to calculate the viscoelastic deformation (Fig.S1). The PSGRN component of this model calculates time-dependent Green's functions for a multi-layered half space. These Green's functions, as well as InSAR surface deformation in LOS direction that is projected to vertical direction using observation incidence angle, are inputs for the PSCMP component to perform the convolution integrations and to compute the time-dependent deformation, geoid and gravity changes with extended fault planes. The two components provide a basis for the least squares estimation of the fractional volume change for each grid block of the model (Vasco *et al.* 2017). This approach is relatively insensitive to the geo-mechanical properties within the reservoir and is able to estimate volume change

across locations that showed significant surface deformation. In this source model, there is no restriction on the number of layers that can be used as an input for a multi-layer subsurface medium. Moreover, the Green's functions database in this model is computed once and can be used repeatedly for modelling deformation with different scenarios if the Earth model remains unchanged. By using a convergence accelerator technique, the computation efficiency will increase and the numerical accuracy of the inverse Laplace transform can be significantly improved by Fast Fourier Transform. Ultimately, PSGRN/PSCMP numerical code can be used for complex geometries and changes at the surface or at a given depth with results in the form of time-series and/or snapshots (Vasco *et al.* 2010).

Table 3. Parameters of the multilayered model including the surface and the upper boundary of the half-space as well as the interfaces at which the viscoelastic parameters are continuous.

No	Depth[km]	Vp[km/sec]	Vs[km/sec]	rho[kg/m^3]
1	00.0	2.9310	1.6922	1709.5
2	0.20	2.9310	1.6922	1709.5
3	0.20	2.7223	1.5717	2106.1
4	0.22	2.7223	1.5717	2106.1
5	0.22	2.8891	1.6680	1913.7
6	0.34	2.8891	1.6680	1913.7
7	0.34	2.9633	1.7108	1526.0
8	0.38	2.9633	1.7108	1526.0
9	0.38	3.7635	2.1728	1885.8
10	0.83	3.7635	2.1728	1885.8
11	0.83	4.0356	2.3300	1847.7
12	1.05	4.0356	2.3300	1847.7
13	1.05	3.7170	2.1460	2480.3
14	10.0	3.7170	2.1460	2480.3

The input parameters which are used to compute the Green's functions include compressional velocity (P-velocity), shear velocity (S-velocity), and density (ρ), all extracted from seismic observations such as sonic logs and density wire-logs. The transient viscosity (η_1), steady-state viscosity (η_2), and the ratio between the effective and the unrelaxed shear modulus (α) will be assumed constant for all subsurface layers (Table3). Layers, which have different parameter values at top and bottom, will be treated as layers with a constant gradient, with a number of homogeneous sublayers. For a Maxwell Body i.e. the transient viscosity (η_1), or the ratio between the effective and the unrelaxed shear modulus, Burger rheology for relaxation of shear modulus is implemented. No relaxation of compressional modulus is considered.

The output of the PSCMP routine includes the time series displacement, stress and tilt components each assigned to their relevant Green's function. In order to estimate volume changes that lead to the observed surface deformation, the reservoir layer is divided into a grid of rectangular blocks. The fractional volume change of each grid block within the layer can be inferred by solving an inverse problem using linear least square approach. This approach works best if a single layer represents the source of volume changes, like those in the Walloon Coal Measures.

Accordingly, for an elastic overburden, the relationship between the displacement vector u_h (that we assumed as predominantly quasi-vertical signal) and the volume changes in the grid blocks ν can be formulated as follows with the certain constraint:

$$u_h = G_h \nu, \quad (2)$$

$$\nu \geq 0\,,$$

where G_h is the vertical Green's function (Vasco *et al.* 1988). The layered model that is used here is the same as the elastic model plotted in Vasco *et al.* (2010). The deformation is associated with volume changes for a grid of rectangular blocks. To solve the inverse problem for volume fluxes in each block, the reflective Newton's method (Coleman and Li, 1996) was used with the minimization of a quadratic function subject to inequality constraint $\nu \geq 0$ (Rucci *et al.* 2010; Rucci *et al.* 2013).

4 RESULTS

4.1 Subsurface Geological Modelling

The surface deformation maps have also proved to be a valuable tool to estimate volume fluxes at reservoir depth (Vasco et al., 2013; Shirzaei et al., 2016) and they can assist with the identification of the subsurface structures where seismic interpretation fails to produce a clear image, such as near surface. Therefore, current study sheds light on the potential of using surface deformation observation and fractional volume change to help with the seismic acquisitions by uncovering the concealed structural faults or changes in the dip direction of underlying formations.

By reviewing the lithology of each well (i.e. petroleum and CSG), eight common stratigraphic units were identified and a simple two-dimensional grid was generated for each of them. The 3D geological

model is comprised of eight stratigraphic horizons: The Early Cretaceous Gubberamunda Sandstone, early to late Jurassic Westbourne Formation, Springbok Sandstone, Walloon Coal Measures, Hutton Sandstone, Evergreen Formation, Precipice Formation, and Basement. Except for few wells, most of the modelled horizons were a close match to the formation tops recorded in the well completion reports. A three-dimensional grid in depth is generated from a grid in time using the predefined velocity model. This three-dimensional grid is then converted to the geological model presented in Fig.4.

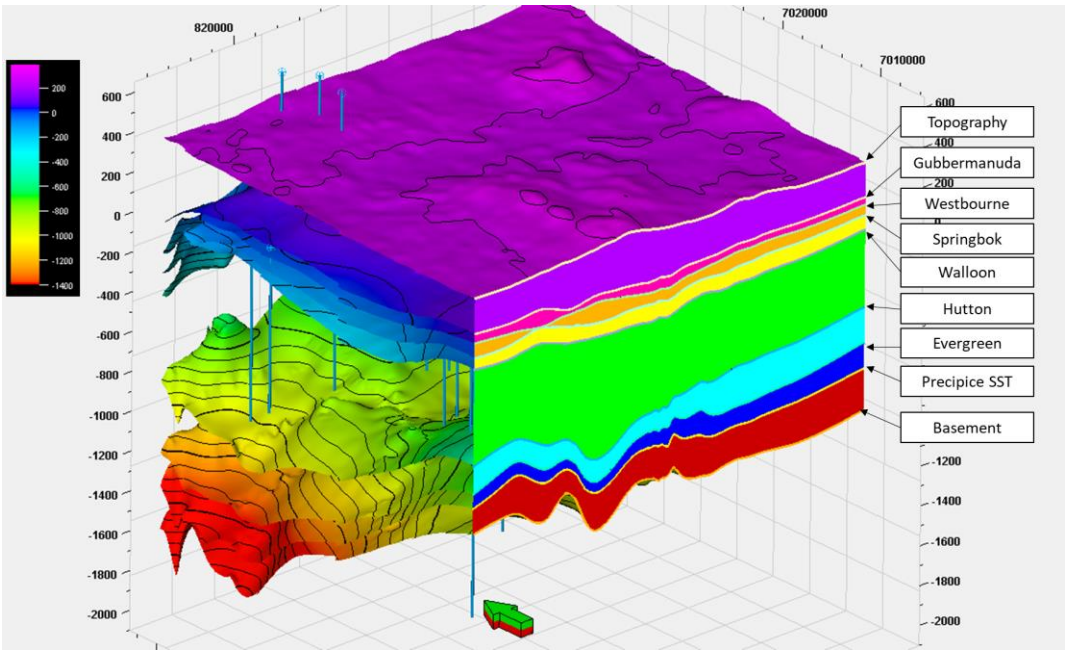

Figure 4. Three-dimensional view of the geological model based on available seismic interpretation and well log data trended with stratigraphic well tops in depth domain.

Fig.5a and Fig.5b show the Gubberamunda Sandstone depth map and the isopach map of Gubberamunda Sandstone-Westbourne Formation interval. The figures show that, both Hutton Sandstone and Evergreen Formation are deep layers (far field) in the deformation region, while other formations act as near-field agents. Moreover, thickness maps over the deformation area show that two zones, i.e. Springbok Sandstone-Walloon Coal Measures and Precipice Sandstone-Basement, have the largest thickness compared to other zones.

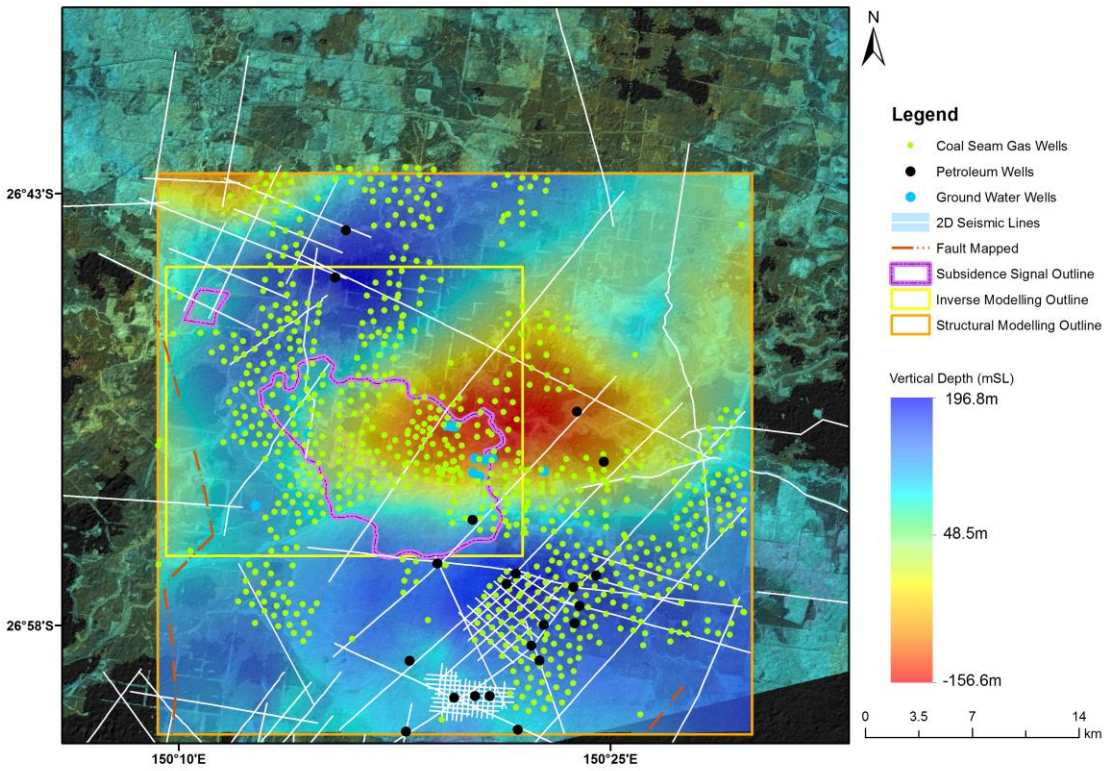

Figure 5(a). Vertical depth map of the Gubberamunda Sandstone formation in the study area. This map is extracted from seismic interpretation and velocity modelling steps.

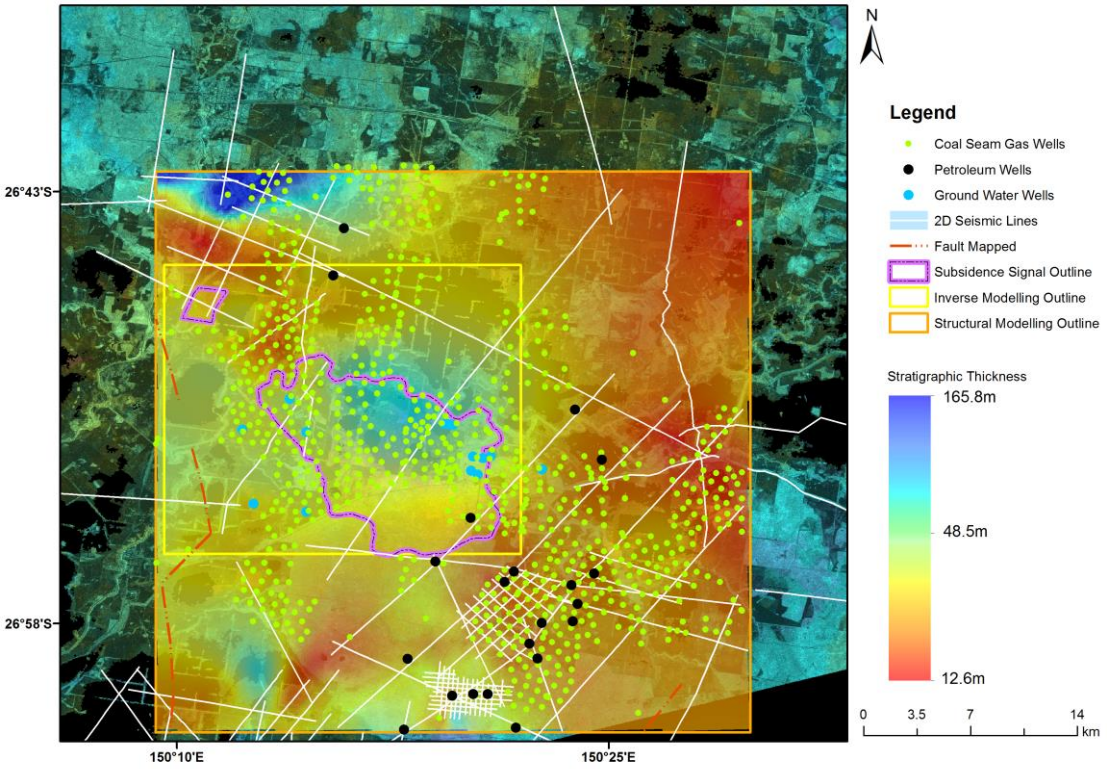

Figure 5(b). Isopach map for the Gubberamunda Sandstone and Westbourne Formation in the study area. This map is extracted from seismic depth conversion.

4.2 Property Modelling

Subsurface rock properties were calculated at well locations using the wireline logs. Kriging was used to interpolate the properties between the wells and within the vertical bounds of the modelled horizons. Kriging relies on the spatial relationship in the dataset that can be recognized through variogram data analysis (Wackernagel, 2010). The goodness of fit for *kriging* is highly dependent on the abundance and spatial distribution of the data available. Despite the under sampled regions in our dataset criteria *kriging* was able to capture the heterogeneity of the system as a viable petrophysical modelling option.

The modelled spatial distribution of acoustic properties shows abrupt changes in the area of study. Fig.6 depicts low range values between 94 and 102msec/ft (~31.30× 10-5sec/m and 33.97× 10-5sec/m) are associated with the Walloon coal-bearing formation. However, compressional velocity (V_p) varies from 2650 to 3200 m/sec within deformation area to less than 2500 m/sec in the south-western part of the study area (Fig.7).

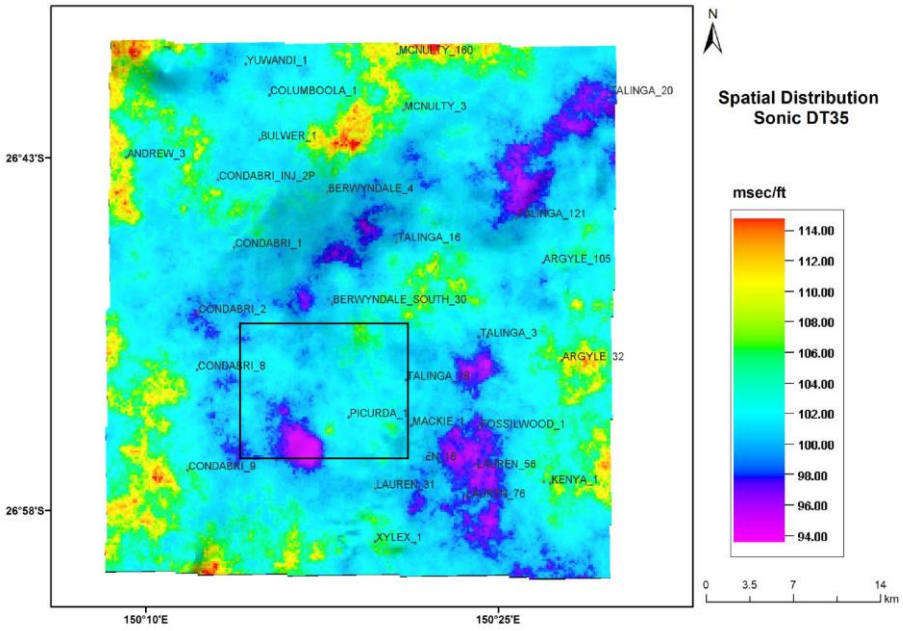

Figure 6. Spatial distribution of sonic log over the entire region within the Walloon Coal Measures layer. As it is shown, the values are the lowest in the proximity of the deformation region and change abruptly from south to north.

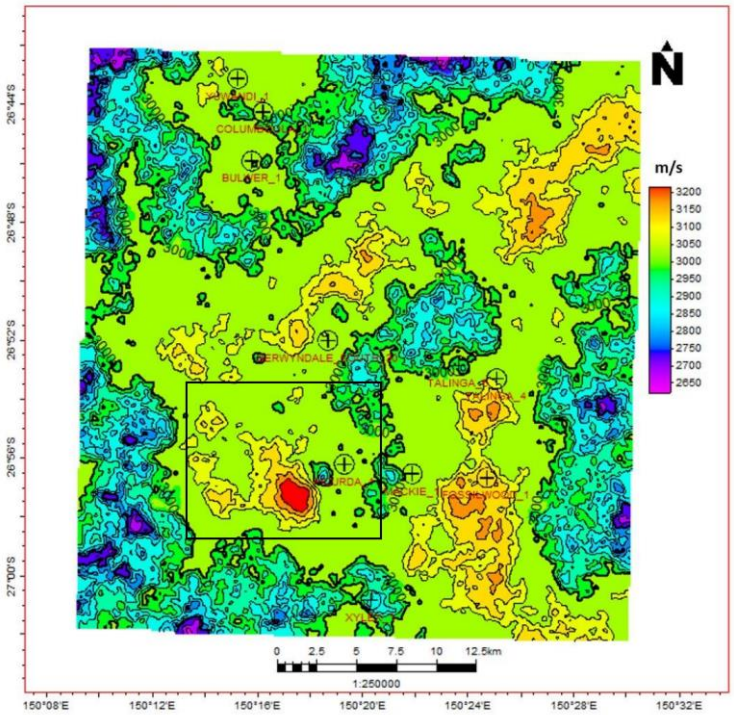

Figure 7. Spatial distribution of average compressional velocity over the entire modelling region within the Walloon Coal Measures-Hutton interval. As it is shown the compressional velocity has the lowest value in the south-western part of the study area, but over the deformation area, the values are quite high.

Within Walloon Coal measures, the neutron porosity values show that the deformation signal is located on an area with porosity values between 31 and 37 PU (porosity unit)(Fig.8). In addition, areas with deformation show medium to high Gamma Ray response corresponding to shale formations (Fig.9) and the relatively higher density ranges of 2.2 to 2.4 g/cm3 (Fig.10).

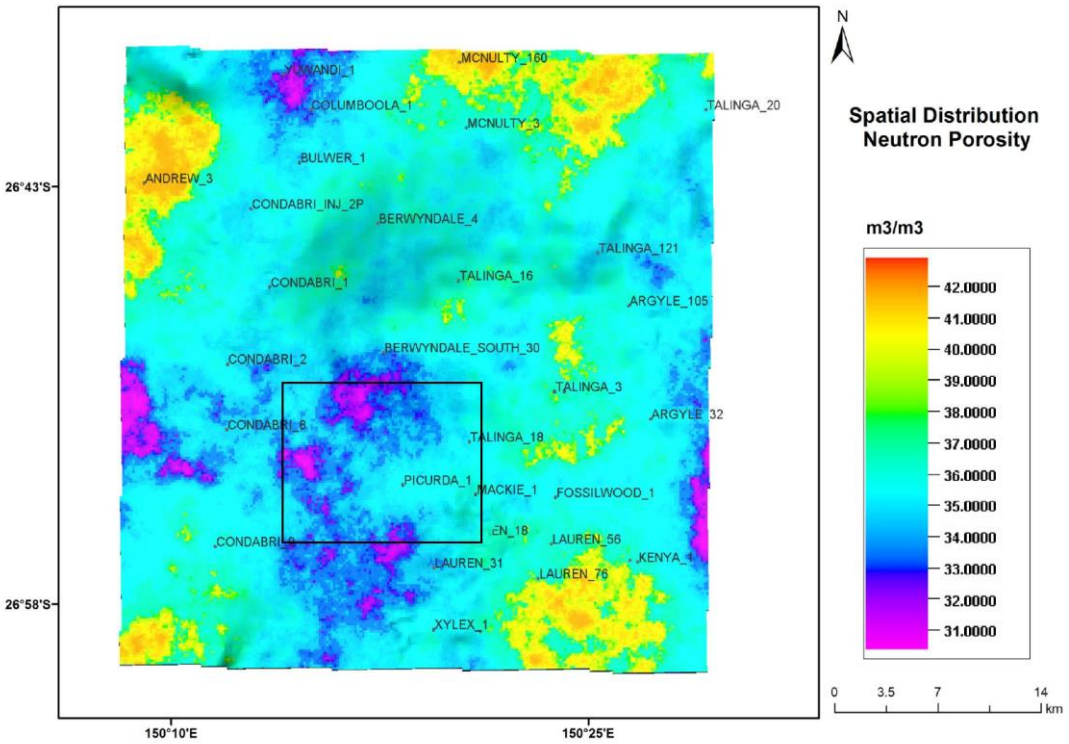

Figure 8. Spatial distribution of neutral porosity over the entire outline for geological modelling. While the majority of study area covered with medium neutral porosity formations, the area with deformation signal shows both high and medium porous formations.

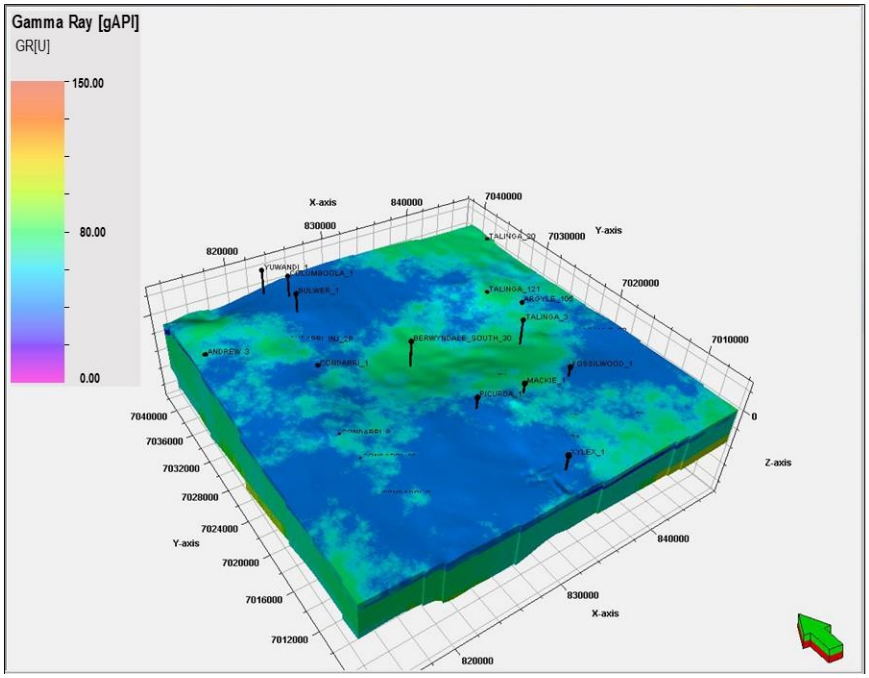

Figure 9. Spatial distribution of gamma ray response in three-dimensional view. It shows that GR values in area with deformation vary between 60 and 100 gAPI.

Compared to these dense areas, the concentration of coal seams is higher in the south-western corner of the study area with low density and high apparent porosity (Fig.10). Although the Spontaneous Potential (SP) distribution is similar in the northern and southern part of the deforming area, with values changing from -200mV up to 300mV, the SP values drop significantly at the centre of the study area, approaching zero. This might indicate that there is an east-west trend for the presence of hydrocarbon bearing formations in the area and that trend may be associated with the regions of deformation (Fig.11).

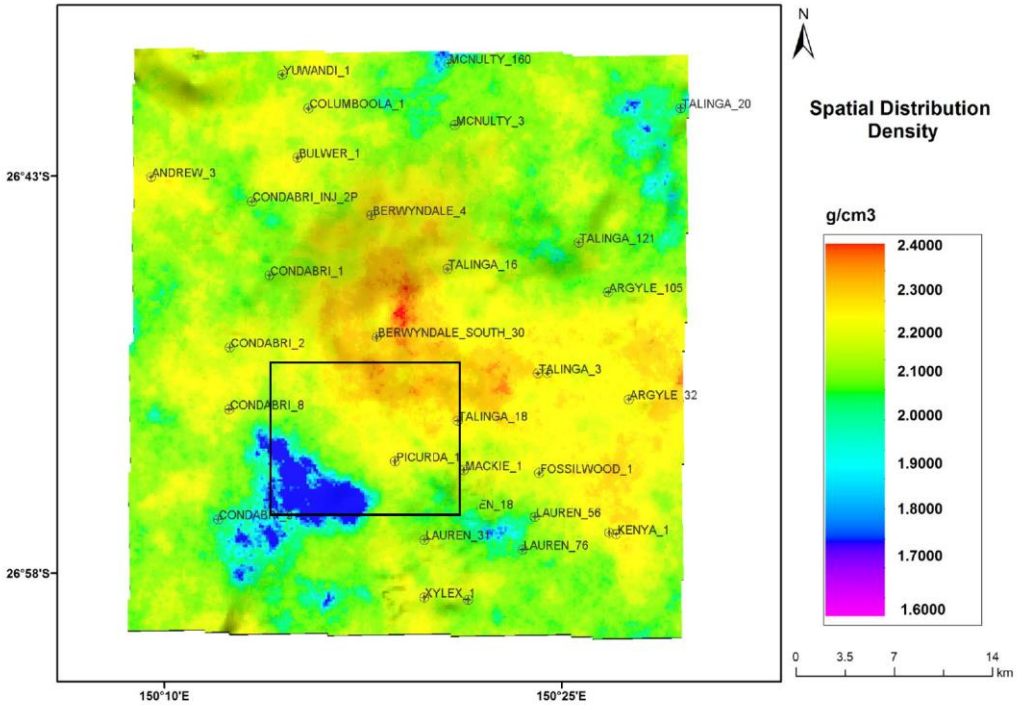

Figure 10. Spatial distribution of density over the modelling area at Walloon Coal Measures (~ -400m depth) in g/cm3 up scaled for the well-bore column in the subsurface model.

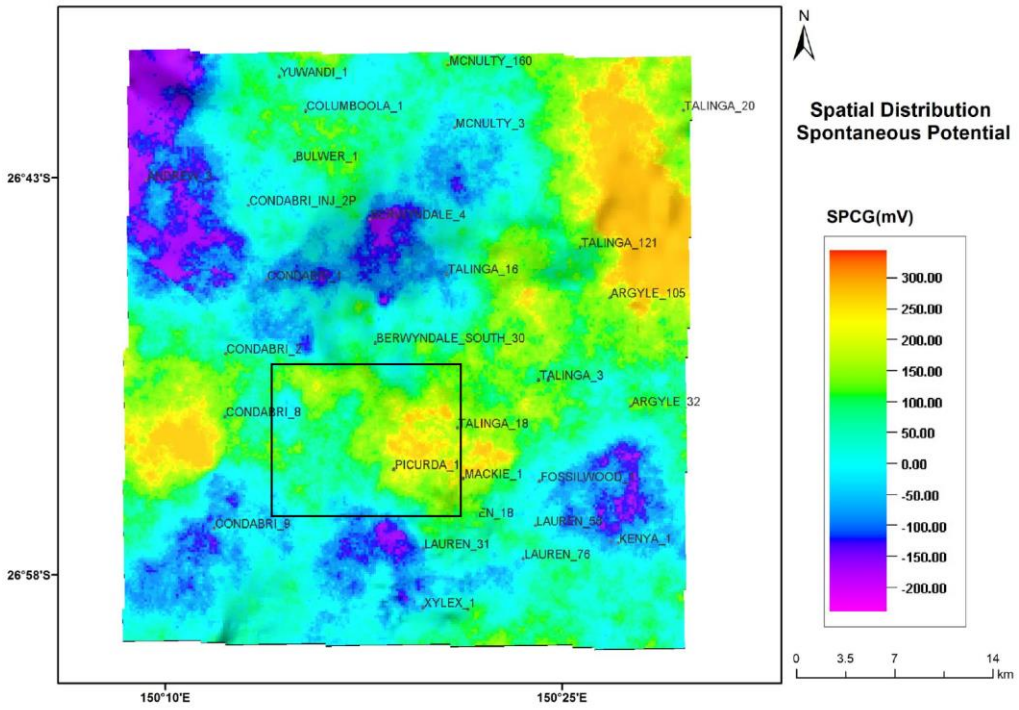

Figure 11. Spatial distribution of Spontaneous Potential (SP) over the outline of modelling with the highest values in the proximity of Condabri_8, Picurda_1, and Talinga_121 within the Walloon Coal Measures.

4.3 Pressure Data Analysis

The pressure-depth plot extracted from CSIRO's Pressure QCTM system (Fig.12) is used to evaluate the formation pressure and to interpret the consequent impact of each data point in the model results. The overall pressure-depth trend of the available downhole measurements in the Surat Basin (solid purple line) is slightly less than the hydrostatic pressure gradient (9 kPa) and far less than the lithostatic (overburden) pressure gradient (2.25 kPa). In other words, the pore pressure is lower than the hydrostatic pressure, indicating that the formations including the reservoir are supported by the matrix and have anomalously low pressure. Deviation from the hydrostatic pressure gradient may be due to natural causes, but it is more likely to be induced by anthropogenic activities, related to either pumping (i.e. groundwater use or CSG production) or fluid injection. In the Surat Basin, eight out of ten petroleum wells that had undergone formation pressure tests in more than one formation show

significant differences in the hydraulic head values in each formation (Hodgkinson *et al.* 2010). However, these wells are out of the study area and are not going to be considered in this study.

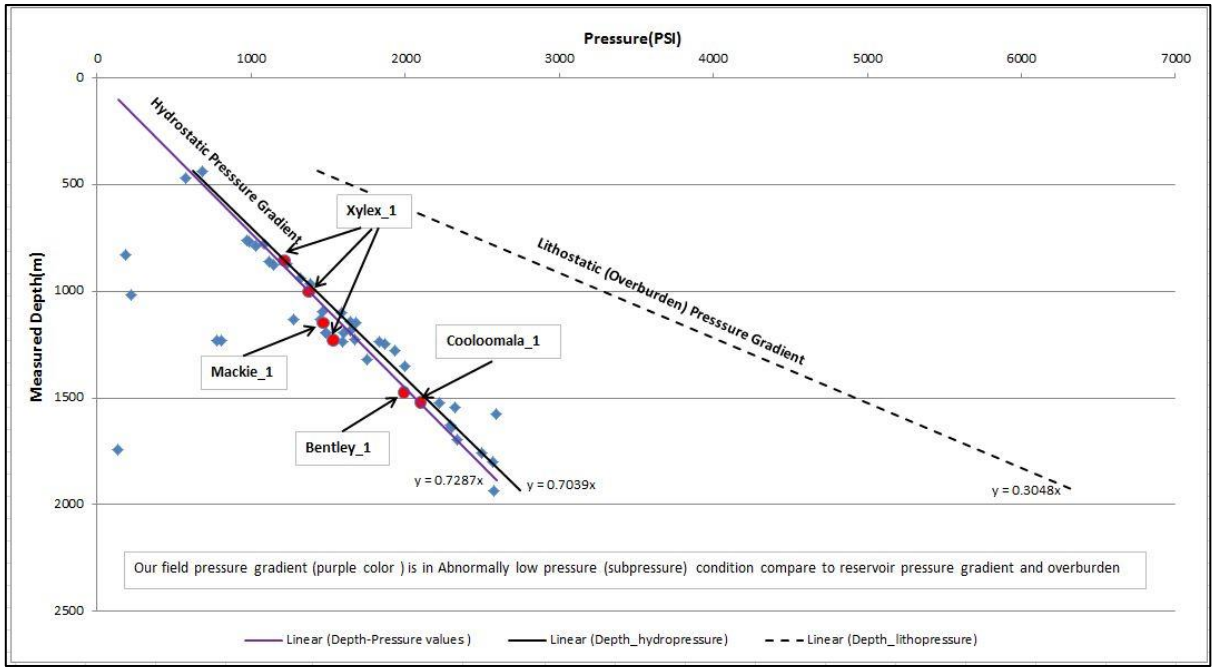

Figure 12. Pressure – Depth gradient plot for 31 petroleum wells available in the entire Surat Basin (solid purple line) and its comparison with standard hydrostatic pressure and lithostatic pressure gradients in a reservoir.

4.4 Geophysical Inverse Modelling

Following the subsurface geomodelling using *in situ* geological, petrophysical, and geophysical datasets in the area of interest, we characterized the structural faults and petrophysical properties within each subsurface formation. Assuming that the subsurface layer undergoing volume change is embedded in a layered elastic medium, we inverted the surface deformation, obtained from space-borne geodetic observations, to estimate fractural volume change. Source characterization is based on a layered elastic model and consists of two parts: inverse modelling, where we estimate the volume changes within the shallow reservoir (i.e. Walloon Coal Measure), and forward modelling to approximate surface deformation based on previously estimated volume change showed in Fig.S1.

For the inverse modelling within the Surat Basin, the model is subdivided into a 30×30 grid of cells in both directions, for an aerial extent of 21km by 21km. The layers of the elastic model extend from the surface to 10 km in depth. Each cell in the source layer may undergo distinct volume change and the relationship between volume change and surface deformation is given by the system of constraints.

Formation depth, formation density, and elastic properties such as compressional velocity and shear velocity are input parameters to the inversion code. The resolution of the inversion procedure or the suitable block size is usually in relation to the spatial averaging inherent in the inversion that is determined by the resolution matrix associated with the inversion procedure. For regularizing the inverse problem, roughness penalty was used with depth and rock type as prior information (Rucci et al., 2013)

Fig.13 shows the fractional volume change calculated for the Walloon Coal Measures using elastic properties of medium. There is also a NW-SE trend for the volume change over the area that is quite stable by changing the depth of source layer and can be seen in the forward modelling results later. Positive values of fractional volume change are probably the result of noise in the InSAR observation signal due to the atmosphere, or ground motion due to shallow processes such as groundwater flow.

In order to examine the sensitivity of the inverse model to its parameterization, two different synthetic tests were executed. In the first test, the depth of Walloon Coal Measure (WCM) was increased from 380m to 780m with increment steps of 100m in the synthetic deformation map; while for the second test, the density of the WCM was variable in a range between 1526kg/m^3 and 1885.8kg/m^3 (Fig.14 and Fig.15). In both tests, *range change data* is the real InSAR observations over the area of interest with the maximum downward movement in the center of the image, and *Forward layer.degrees.calc* is the synthetic deformation map extracted from the forward modelling exercise. Residual maps in Fig.16 show that by changing the reservoir depth, the absolute residual values in the centre and lower right corner of the image increase, while the centre of the image displays negative residuals and the lower right corner has positive residuals. On the other hand, variation in density of coal formation resulted in positive residuals in the lower right corner of the image indicating that an increase in formation density decreases the surface deformation rate (Fig.17). According to synthetic tests and the residual maps, increasing the density of CSG reservoir (i.e. WCM) layer from 1526 (kg/m3) to 1836(kg/m3) changes the subsidence values only slightly and in a reverse fashion. Similarly, changing the depth of the source layer from 380m to 780m will cause a minor increase in the downward motion. We conclude that variations in density and depth of the shallow reservoir layer will not significantly change the deformation in the forward model.

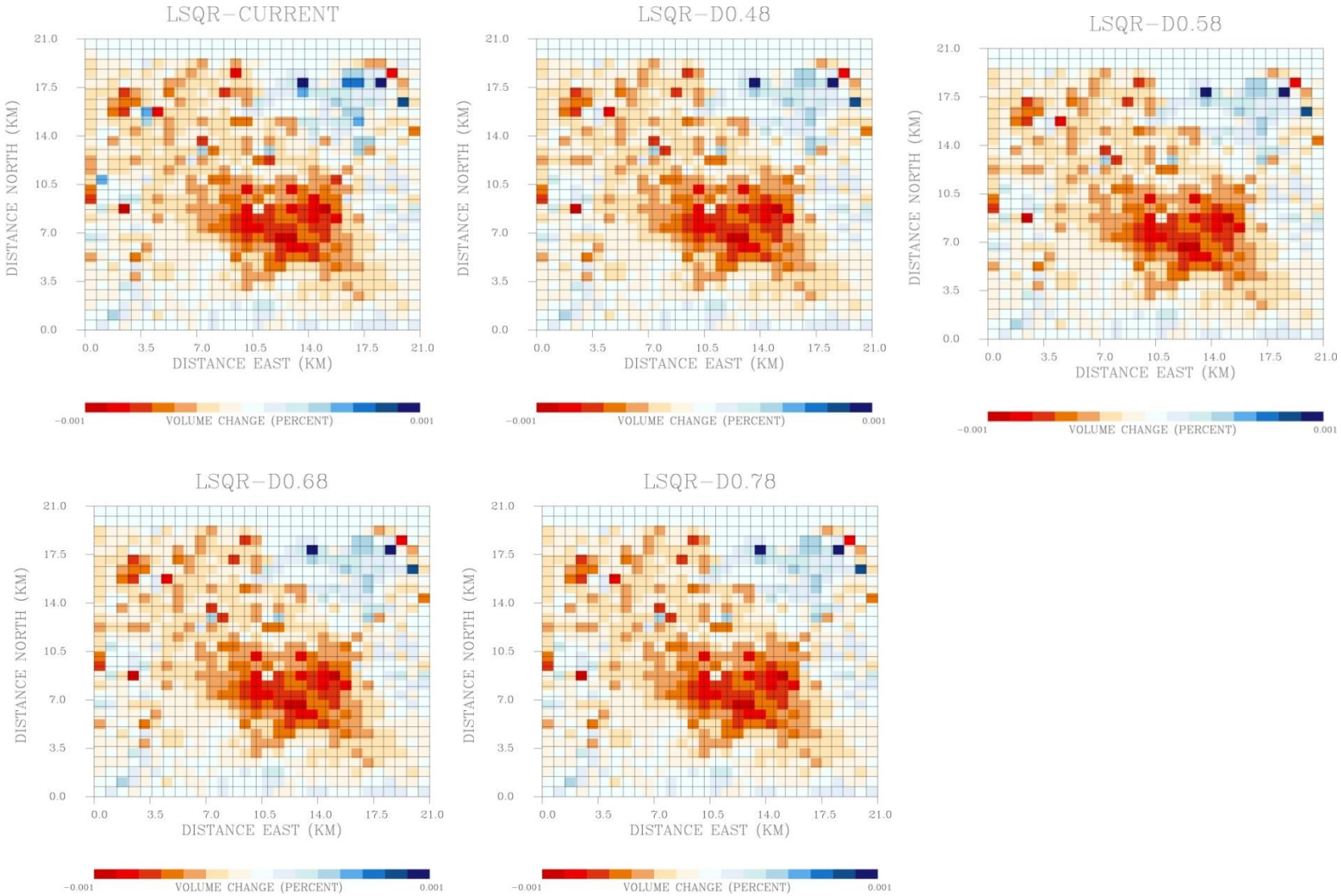

Figure 13. Result of modelling as a fractional volume change (equates to change in volume over initial volume) represents the source as a grid that undergoes variable volume changes. As it is shown changing in the depth of reservoir (WCM) from 0.38 km to 0.78 km did not impact on the amount of volume flux significantly.

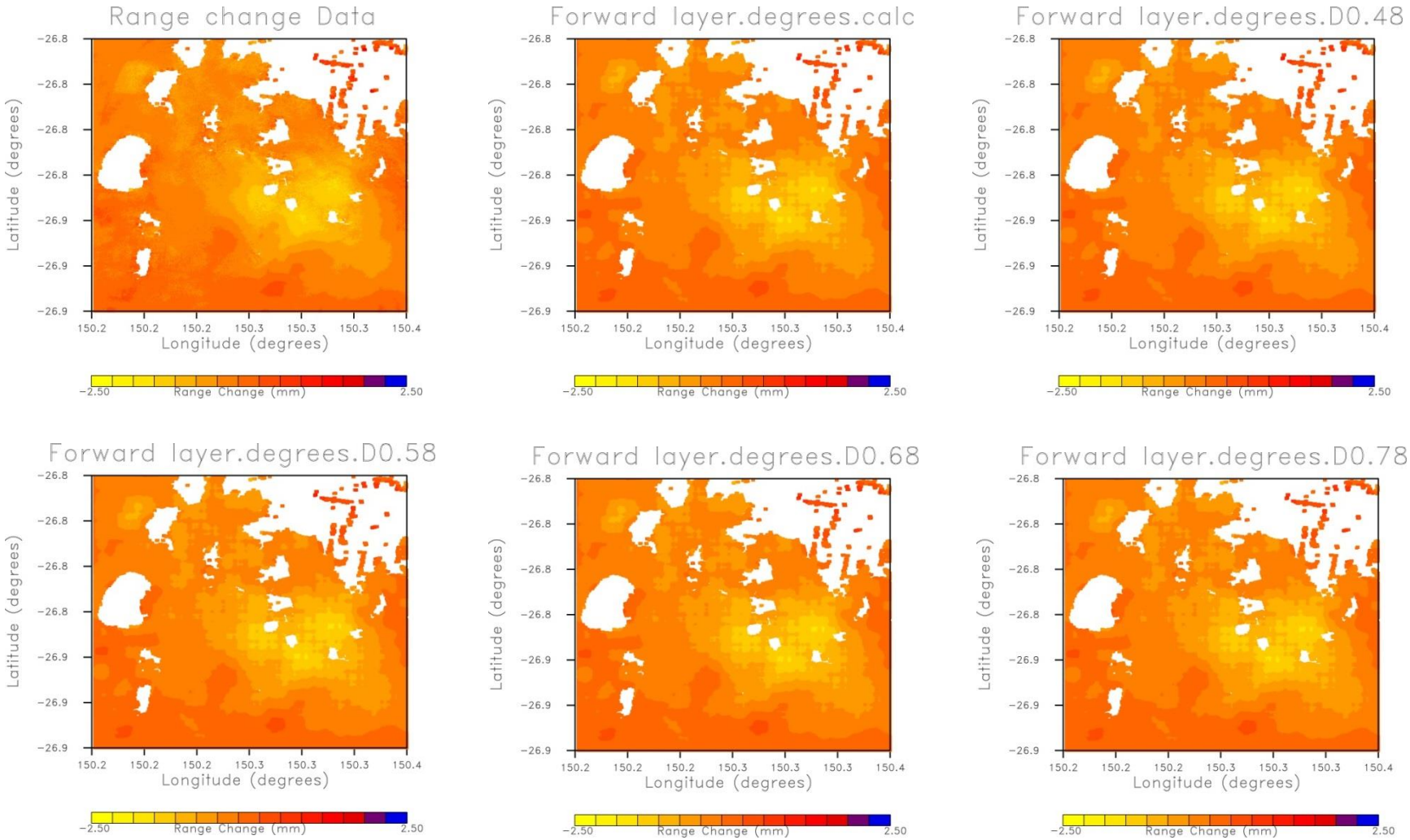

Figure 14. The impact of different depths of Walloon Coal Measures (CSG reservoir) on the rate of surface deformation recovery. Range change data is surface deformation observation by SAR interferometry (truth) while others are the outcomes of forward modelling (simulated).

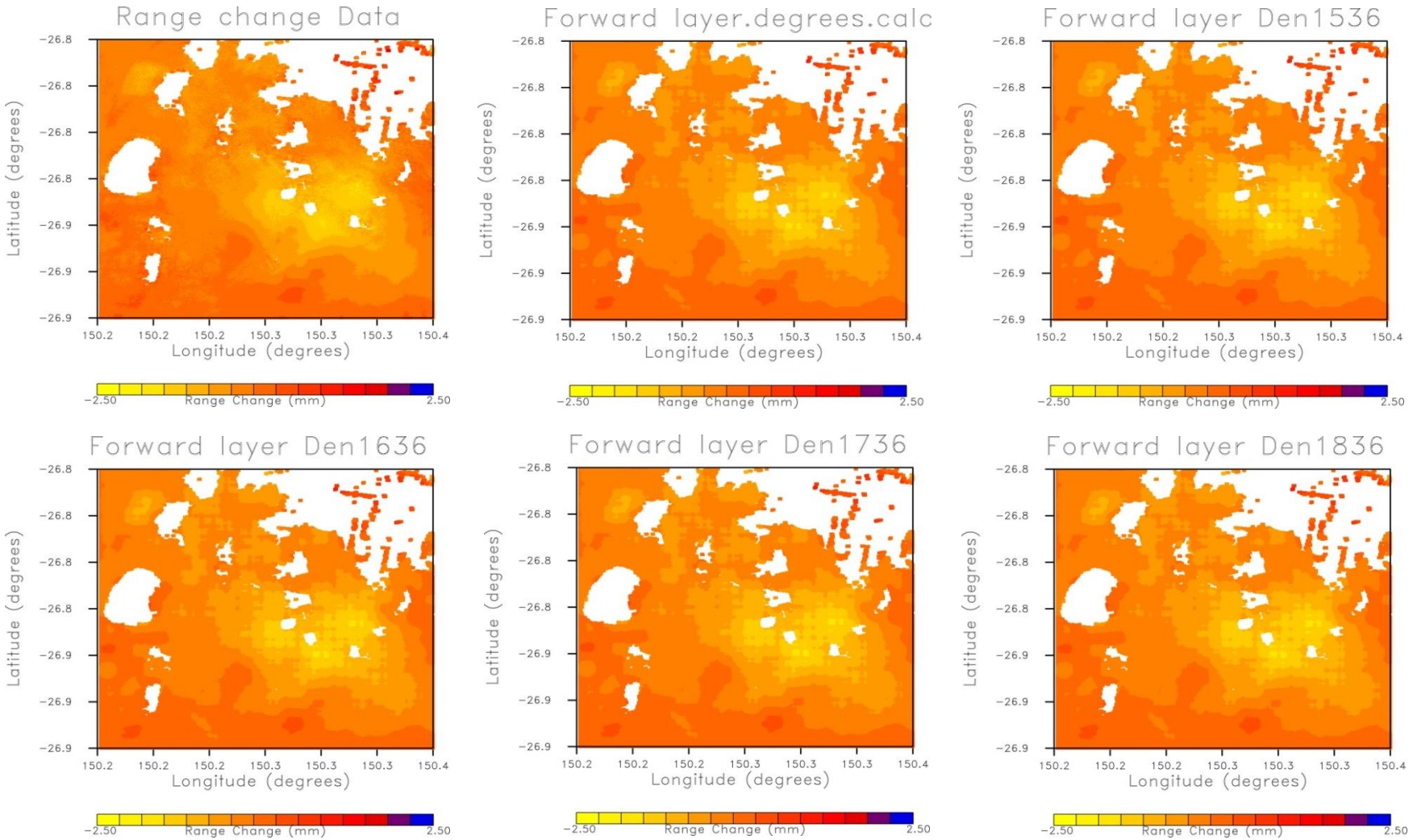

Figure 15. The impact of different formation density of Walloon Coal Measures (CSG reservoir) on the rate of surface deformation recovery. Range change data is surface deformation observation by SAR interferometry (truth) while others are the outcomes of forward modelling (simulated).

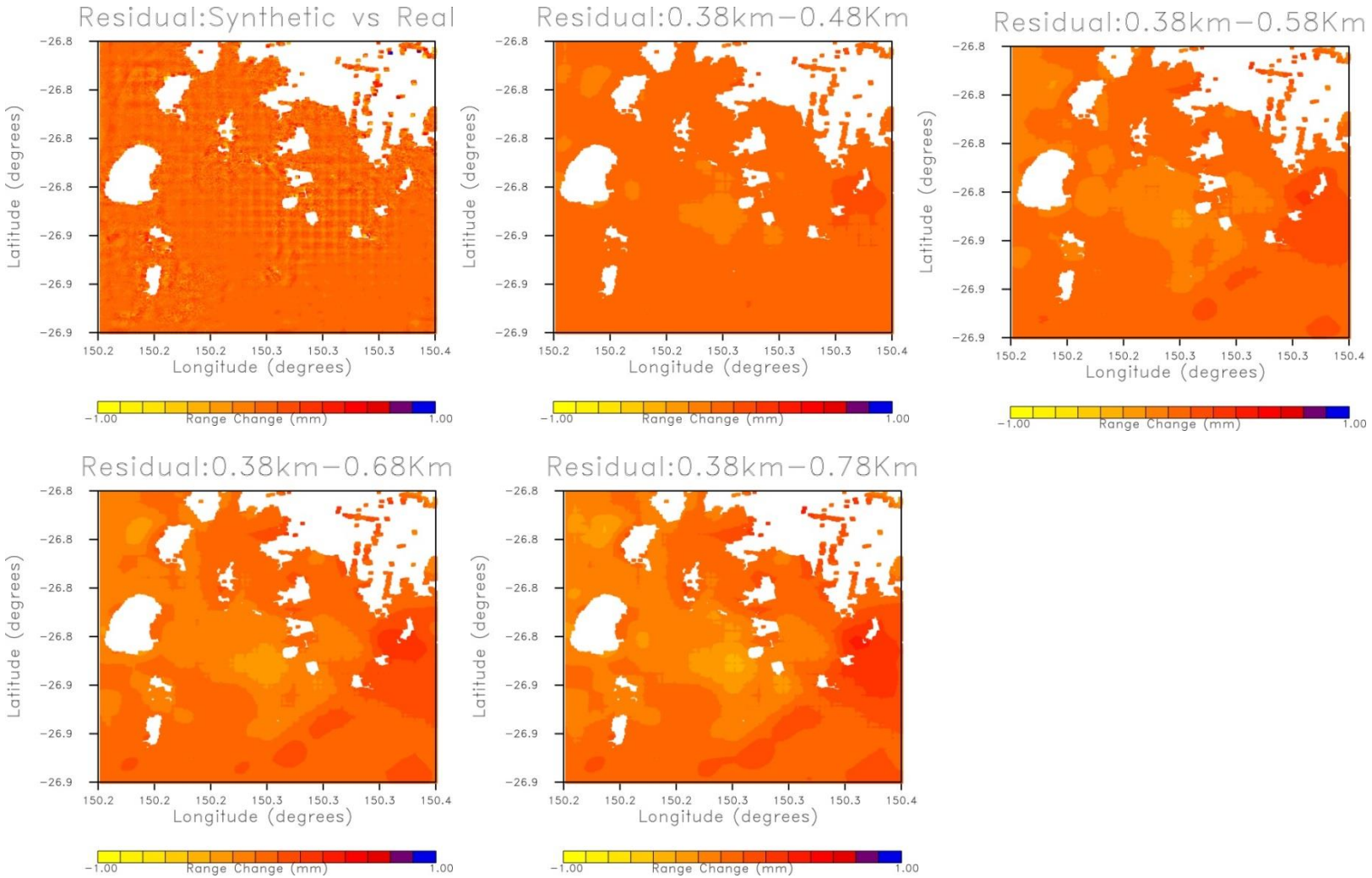

Figure 16. Residual values between synthetic deformation maps at different depths of Walloon Coal Measure source layer. Based on seismic interpretation and 3D modelling, Walloon Coal Measure is located at 380m depth.

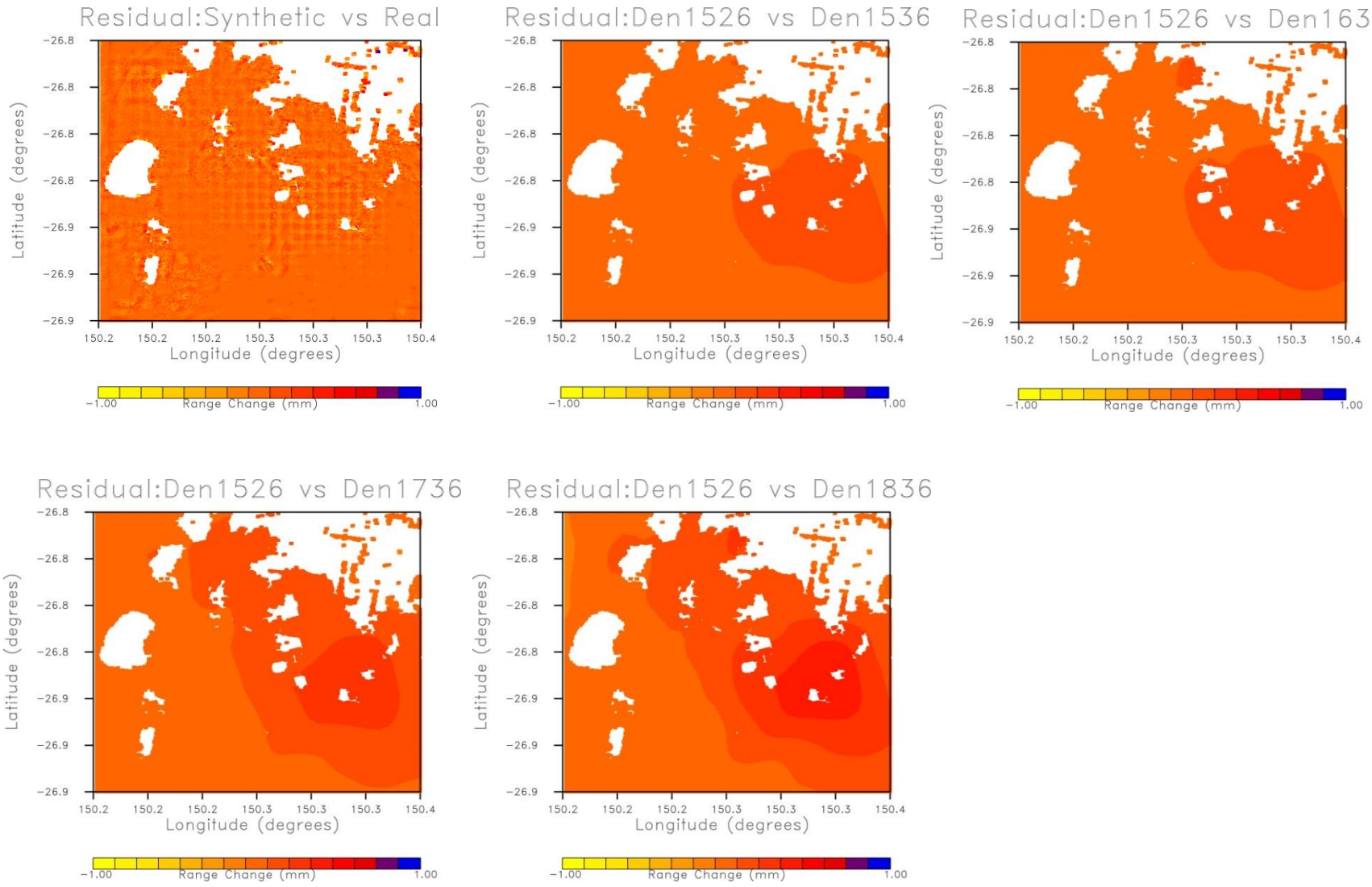

Figure17. Residual values between synthetic deformation maps for different densities of Walloon Coal Measure source layer. Based on seismic interpretation and 3D modelling, density of Walloon Coal Measure changes between 1526(kg/m3) and 1885.8 (kg/m3).

5 DISCUSSION

The fluid that is extracted from or injected into a reservoir leads to pressure and volume changes within the host formation, resulting in deformation within the overburden, and stress changes in the region surrounding the reservoir. Therefore, once volume changes are computed, they can be mapped into pressure changes through a linear transformation (Rucci *et al.* 2013).

In this paper, a numerical method was used to mimic subsurface stratigraphic units and structural features with their petrophysical properties. Extracting subsurface stratigraphic layers was mainly based on interpolating between the available 2D seismic sections tied with petroleum well tops.

For the sake of property modelling, CSG wire-line information was sufficient to conduct a petrophysical analysis. According to these analyses, the deformation signal is located over a porous medium composed of a shale formation that has the potential to bear hydrocarbon and not that much coal. In addition, the compressional velocity in areas with deformation is quite high in comparison with other areas in the outline. Moreover, the thickness of different formations for this specific area according to isopach maps is significantly variable from medium to high in Precipice Sandstone - Basement zone to very low in Evergreen formation - Precipice Sandstone zone. Using depth and isopach maps extracted from the three-dimensional geological model, we see that from the surface up to the Walloon Coal Measures, a major reservoir for unconventional gas, layers are shallow and their thickness is variable, which is compatible with the aquifer-aquitard nature of the subsurface in this particular area of the Great Artesian Basin.

Considering the fact that the proposed area is located in a region of low relief, with several stratified layers, and the reservoir layer is embedded in a stratified elastic medium, a multi-layer viscoelastic geophysical inverse model was chosen (Vasco *et al.* 2008) to estimate fractional volume change. For this inversion, subsurface properties such as compressional velocity, shear velocity, depth, and density were extracted from the static geological model. This geological model consisted of eight subsurface stratigraphic units with intersecting structural features. According to the extracted properties for each

formation, the area with the maximum rate of surface deformation is located over a porous medium with quite high compressional seismic velocity.

To measure the sensitivity of the model to any changes from its initial state, the depth and density of the reservoir strata were then varied and the residuals of the surface deformation rate for both real and synthetic datasets were calculated. The residual maps show that slight changes in depth of the CSG layer will increase the absolute residual values both in downward and upward motions, but variations in density of this layer resulted in declining surface deformation rate due to compaction. However, the magnitude of these variations is not significant, and we are able to obtain an accurate estimate of the model parameters using the available InSAR data.

Although the majority of volume change occurred in the center of the image with maximum surface deformation rate. As shown in Fig.18, there is a NW-SE trend of volumetric flux and its two-lobe pattern over the Walloon Coal Measures depth map, supporting the controlling effect of an underlying fracture or fault for reservoir geo-mechanical behavior. From the geological modelling, it was already known that the general slope of the formations in this part of the Surat Basin is towards the South-West. The asymmetric size of these lobes indicates that the slope gradient of the formations in this part of the Surat Basin might be liable for such a pattern when there is limited CSG well available over the western part of the volumetric change. Therefore, resource extraction with a dense network of CSG wells on the eastern side of the volumetric change is suggested as a potential cause for the detected surface settlement and the subsequent volume change but for the western side, tectonic elements are more likely to be the controlling factor for the signal. Unfortunately, due to the lack of seismic lines or other ancillary in-situ measurements in the center of deformation area, independent study for verifying these assumptions was not possible, but the effects of a distinct fracture or fault can be clearly observed in the middle of the deformed area. Therefore, the inversion of deformation fields for volume change derived from InSAR observations is a promising technique for the identification of geological structures, such as faults, that were not mapped previously using field observations or seismic interpretation.

6 CONCLUSION AND FUTURE PERSPECTIVES

InSAR-based deformation maps in the Surat Basin (Moghaddam *et al.* 2016) highlighted areas with a significant risk of ground failure over a three-year observation period. By interpreting available two-dimensional seismic surveys in the time domain and then tying them to well-log depth measurements, a three-dimensional geological model of the deformation area and its vicinity was developed. Using a suitable velocity model, this static geological framework was then converted from the time to depth domain and was improved by inserting petrophysical attributes for further geological and geophysical analysis. Elastic properties of each subsurface formation and the rate of ground surface deformation were then combined to estimate variations in reservoir volume changes and to define the subsurface structural behavior at the local scale.

According to the results obtained from three-dimensional geological modelling and geophysical inverse modelling of InSAR data for estimating volume change, fluid withdrawal with a dense network of CSG wells is the most likely source of the observed surface deformation. However, the impact of structural faults and tectonic framework as constraining barriers also appears to be an important contributing factor. Formation properties such as depth, density, and formation slope were also initially hypothesized as a third source, but testing the impact of changing these properties on the rate of deformation suggested otherwise. Although residual maps revealed that the marginal change in reservoir depth will increase the absolute residuals, and variations in its density will have the opposite effect on deformation rate, the impact of these factors was found to be negligible for the extracted fractional volume change.

This research presents several new contributions, such as applying viscoelastic multi-layer source model (Vasco *et al.* 2008) to an unconventional hydrocarbon reservoir i.e. CSG and evaluating the role of reservoir volumetric change in detecting subsurface structural features such as faults. The proposed source model was previously used for both earthquake epicenters and for conventional hydrocarbon resources such as oil and gas but has never been tested for stratified layers of shallow reservoirs such as CSG.

The surface deformation maps have also proved to be a valuable tool to estimate volume fluxes at reservoir depth and an indicator for subsurface structures that were not detected through seismic means. Therefore, the main contribution of this paper is proposing a novel view on using ground surface deformation without taking account the location of local faults. Volumetric change estimation using InSAR inversion was able to accurately map the location of available faults that can be used to resolve uncertainties of imaging geology and to constraint subsurface geological models where poor seismic data coverage exist.

According to this study and previously published articles, the fractional volume change approximates compaction or expansion in a rock matrix associated with fluid flow. In the case of CSG mining, it could be the coupled impact of pressure change in both the coal layer and the fresh-water shallow aquifers. Increasing the overburden pressure on a relatively thin coal layer can be projected as a ground deformation on the surface. Accordingly, a comprehensive geo-mechanical model to differentiate these causative effects needs to be built to explicitly define the impact of each potential cause in the region (i.e. groundwater extraction, CSG mining, fluid migration and soil shrinkage) that might be responsible for the reported rate of deformation, and the subsequent volume change at reservoir depth.

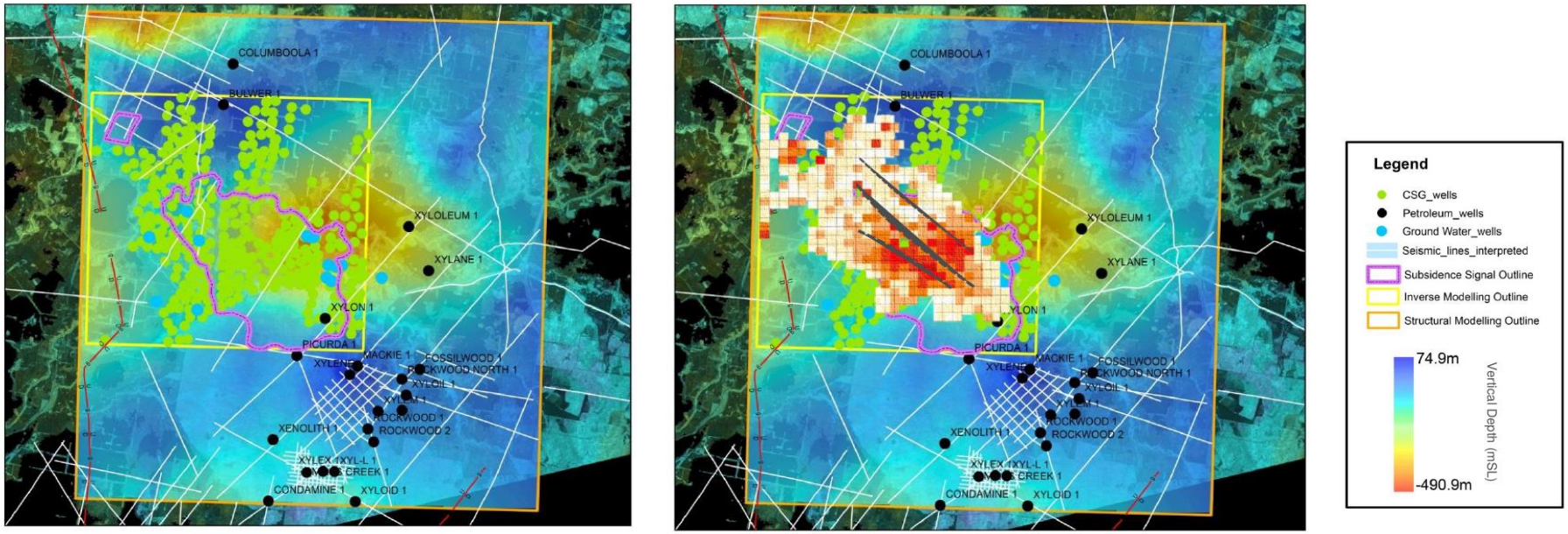

Figure18. (a) Location map of all in-situ measurements including groundwater, petroleum and CSG wells along with the distribution of interpreted seismic lines. (b) The result of geophysical inverse modelling using InSAR surface observation superimposed on shallow reservoir layer i.e. the Walloon Coal Measure depth map.

7 DATA AVAILIBILITY

Dataset related to this article can be accessed as an open-source online data hosted at different repositories. Aquifer and groundwater historical data products including water quality information provided by the State of Queensland (Department of Natural Resource, Mines and energy) [2015]. These datasets can be accessed through contacting qdexsupport@dnrme.qld.gov.au. Well Completion Reports and check shots for several wells were obtained from Queensland Gas Company (QGC) [2006-2011], Australia Pacific LNG [2011], Union Oil Development Corporation [1964] that are open files and publically available. ALOS PALSAR L-band satellite acquisitions were provided through a Japan Aerospace Exploration Agency (JAXA) and Ministry of Economy, Trade and Industry METI project (P1338002) and processed using GAMMA software. For 3D geological modelling Petrel E&P software platform developed by Schlumberger was used while geophysical inverse modelling was mainly completed by applying open-source code developed by Donald W. Vasco and the PSGRN/PSCMP code available at GFZ Potsdom http://gfzpublic.gfz-potsdam.de/. Pressure Plot V2.1.1 software developed by CSIRO and can be accessed as an open-source software via CSIRO's website.

Acknowledgments

ALOS PALSAR L-band acquisitions were provided through Japan Aerospace Exploration Agency (JAXA) and Ministry of Economy, Trade and Industry METI project (P1338002). The authors would like to thank the FrontierSI (formerly the CRC for Spatial Information) for providing access to InSAR processing software and 3D Geo Pty Ltd. for providing access to Petrel geological modelling software. Finally, the support from the Geological Survey of Queensland, the Department of Natural Resource, Mines and Energy (DNRME), and Geoscience Australia for accessing to in situ measurements and open files is gratefully acknowledged. An International Postgraduate Research Scholarship (IPRS) and Australian Postgraduate Award of Monash University, Melbourne, Australia financially supported this work.

REFERENCES

Al-Khalifa, T., Tobias, M.A., Payenberg, H.D., Lang, S.C., 2007. Overcoming the Challenges of Building 3D Stochastic Reservoir Models Using Conceptual Geological Models – A case study. SPE Middle East Oil and Gas Show and Conference, SPE- 104496. https://doi.org/10.2118/104496-MS.

Adeoti, L., Onyekachi, N., Olatinsu, O. , Fatoba, J., Bello, M., 2014. Static reservoir modelling using well log and 3D seismic data in a KN Field, offshore Niger Delta, Nigeria, International Journal of Geosciences, 5, 93-106.

Badley, M. E. 1985. Practical Seismic Interpretation, Prentice Hall, NJ, USA.

Cameron, M., Fomel, S., Sethian, J., 2006. Seismic velocity estimation and time to depth conversion of time-migrated images paper presented at SEG Annual Meeting, New Orleans, USA.

Coleman, T. F., Li, Y., 1996. A Reflective Newton Method for Minimizing a Quadratic Function Subject to Bounds on Some of the Variables, SIAM Journal on Optimization. 6(4), 1040-1058. https://doi.org/10.1137/S1052623494240456.

Du, Y., Aydin, A., Segall, P., 1992. Comparison of various inversion techniques as applied to the determination of a geophysical deformation model for the 1983 Borah Peak earthquake, Bulletin of the Seismological Society of America, 82(4), 1840-1866.

Ezekwe, J. N. 2011. Petroleum Reservoir Engineering Practice, Prentice Hall, Upper Saddle River, NJ,USA.

Ezekwe, J. N., Filler, S. L., 2005. Modelling Deepwater Reservoirs in Annual Technical Conference and Exhibition, SPE 95066, Dallas, TX, USA.

Fallara, F., Legault, M., & Rabeau, O., 2006. 3-D Integrated Geological Modelling in the Abitibi Sub province (Quebec, Canada): Techniques and Applications, Exploration and Mining Geology. 15(1-2), 27-41. https://doi.org/10.2113/gsemg.15.1-2.27.

Hodgkinson, J., Hortle, A., McKillop, M., 2010. The application of hydrodynamic analysis in the assessment of regional aquifers for carbon geostorage: Preliminary results for the Surat Basin, Queensland, APPEA Journal. 50(1), 445-462. https://doi.org/10.1071/AJ09027.

Hosseini, S. A., Lashgari, H., Choi, J. W., Nicot, J.-P., Lu, J., Hovorka, S. D., 2013. Static and dynamic reservoir modeling for geological CO2 sequestration at Cranfield, Mississippi, U.S.A, International Journal of Greenhouse Gas Control, 18, 449-462.

Mallet, J. L., 2008. Numerical Earth Models (EET 3), EAGE Publications.

Martin,M.A., Wakefield, M., MacPhail, M.K., Pearce,T., Edwards,H.E., 2013. Sedimentology and Stratigraphy of an Intra-cratonic Basin Coal Seam Gas Play: Walloon Subgroup of the Surat Basin, Eastern Australia, Petroleum Geoscience.19, 21-38. https://doi.org/10.1144/petgeo2011-043

McCarthy, P., Brand, J., Paradiso, B., Ezekwe, J. N., Wiltgen, N., Bridge, A., Willingham, R., Bogaards, M., 2006. Using Geostatistical Inversion of Seismic and Borehole Data to Generate Reservoir Models for Flow Simulations of Magnolia Field, Deepwater Gulf of Mexico, SEG Technical Program Expanded Abstracts: 1351-1354. https://doi.org/10.1190/1.2147937.

Moghaddam, N.F., Samsonov, S.V., Rüdiger, C., Walker, J.P., Walter, D., Hall, M., 2016. Multi-temporal SAR observations of the Surat Basin in Australia for deformation scenario evaluation associated with man-made interactions. Environmental Earth Sciences, 75:282. https://doi.org/10.1007/s12665-015-4864-y.

Queensland Water Commission (QWC), 2012. Underground Water Impact Report for the Surat Cumulative Management Area, Open File Rep., Coal Seam Gas Water, Queensland Water Commission.

Rucci, A., Vasco, D.W., Novali, F., 2013. Monitoring the geologic storage of carbon dioxide using multicomponent SAR interferometry, Geophysical Journal International, 193(1), 197–208. https://doi.org/10.1093/gji/ggs112.

Rucci, A., Vasco, D.W., Novali, F., 2010. Fluid pressure arrival-time tomography: Estimation and assessment in the presence of inequality constraints with an application to production at the Krechba field, Algeria, Geophysics, 75(6), O39-O55. https://doi.org/10.1190/1.3493504.

Samsonov, S., Van der Kooij, M., Tiampo, K., 2011. A simultaneous inversion for deformation rates and topographic errors of DInSAR data utilizing linear least square inversion technique, Computers & Geosciences, 37(8), 1083-1091.

Shirzaei, M., Ellsworth, W.L., Tiampo, K.F., Gonzalez, P.J., Manga, M., 2016. Surface uplift and time-dependent seismic hazard due to fluid injection in eastern Texas. Science 353(6306), 1416-1419.

Singh, V., Yemez, I., Sotomayor, J., 2013. Key factors affecting 3D reservoir interpretation and modelling outcomes: Industry perspectives. British Journal of Applied Science & Technology. 3 (3), 376-405.

Tiab, D., Donaldson, E. C., 2012. Petrophysics: theory and practice of measuring reservoir rock and fluid transport properties, Gulf professional publishing.

Vasco, D. W., Harness, P, Pride, S., Hoversten, M., 2017. Estimating fluid-induced stress change from observed deformation, Geophysical Journal International. 208(3), 1623-1642. https://doi.org/10.1093/gji/ggw472

Vasco, D. W., Datta-Gupta, A., 2016. Subsurface Fluid Flow and Imaging, Cambridge University Press, Cambridge.

Vasco, D. W., Rutqvist, J., Ferretti, A., Rucci, A., Bellotti, F., Dobson, P., Oldenburg, C., Garcia, J., Walters, M., Hartline, C., 2013. Monitoring deformation at the Geysers Geothermal Field, California using C-band and X-band interferometric synthetic aperture radar, Geophysical Research Letters, 40, 2567-2572, doi: 10.1002/grl.50314.

Vasco, D. W., Rucci, A., Ferretti, A., Novali, F., Bissell, R. C., Ringrose, P. S., Mathieson, A. S., Wright, I. W., 2010. Satellite-based measurements of surface deformation reveal fluid flow associated with the geological storage of carbon dioxide, Geophysical Research Letters, 37(3). https://doi.org/10.1029/2009GL041544.

Vasco, D. W., Ferretti, A., Novali, F.,2008. Estimating permeability from quasi-static deformation: Temporal variations and arrival time inversion, Geophysics, 73, O37-O52. https://doi.org/10.1190/1.2978164.

Vasco, D. W., Johnson, L. R., Goldstein, N. E., 1988. Using surface displacement and strain observations to determine deformation at depth, with an application to Long Valley Caldera, California, Journal of Geophysical Research: Solid Earth, 93(B4), 3232-3242. https://doi.org/10.1029/JB093iB04p03232.

Wackernagel, H., 2010. Multivariate Geostatistics, An Introduction with Applications, Springer.

Wang, R., Lorenzo-Martín, F., Roth, F., 2006. PSGRN/PSCMP—a new code for calculating co- and post-seismic deformation, geoid and gravity changes based on the viscoelastic-gravitational dislocation theory, Computers & Geosciences, 32(4), 527-541. https://doi.org/10.1016/j.cageo.2005.08.006.

Wickens, H. D., Bouma, A. H., 2000. The Tanqua Fan Complex, Karoo Basin, South Africa- Outcrop Analog for Fine-Grained, Deepwater Deposits, in Fine-Grained Turbidite Systems, edited by A. H. Bouma, Stone, C.G., 153-163, AAPG Memoir 72/SEPM Special Publication

Yilmaz, Ö., 2001. Seismic Data Analysis: Processing, Inversion, and Interpretation of Seismic Data, Society of exploration geophysicists.